Low Pressure Plasma Immersion Ion Implantation of Silicon

Zhi-Neng Fan, Qing-Chuan Chen, Paul K. Chu, *Member, IEEE,* and Chung Chan *Fellow, IEEE*

***Abstract*—Mono-energetic plasma immersion ion implantation (PIII) into silicon can be attained only under collionless plasma conditions. In order to reduce the current load on the high voltage power supply and modulator and sample heating caused by implanted ions, the plasma pressure must be kept low (<1 mtorr). Low pressure PIII is therefore the preferred technique for silicon PIII processing such as the formation of silicon on insulator. Using our model, we simulate the characteristics of low pressure PIII and identify the proper process windows of hydrogen PIII for the ion-cut process. Experiments are conducted to investigate details in three of the most important parameters in low pressure PIII: pulse width, voltage, and gas pressure. We also study the case of an infinitely long pulse, that is, dc PIII.**

***Index Terms*— Plasma immersion ion implantation, semiconductor processing, silicon.**

I. Introduction

PLASMA immersion ion implantation (PIII) is a fledgling technique in semiconductor processing [1]–[4]. The major applications include shallow junction formation [5], [6], hydrogenation of flat panel display (FPD) materials [7], and synthesis of silicon-on-insulator (SOI) wafers [8]–[15]. The implantation conditions of different applications are quite different. For instance, shallow junction formation and passivation of FPD require low energy PIII and multiple species implantation, i.e., an in-depth elemental distribution showing more than one peak, can be tolerated. On the other hand, in SOI processes such as separation by plasma implantation of oxygen (SPIMOX) and ion-cut/wafer bonding, the implantation energy is much higher and typically in the 20–100 keV regime. Moreover, in order to form a single buried insulator in the case of SPIMOX or a uniform transferred layer in the case of ion-cut/wafer bonding, the implantation energy must be tightly controlled and it is highly preferred that only one ion species be implanted. Since beam filtering is absent in PIII, all species existing in the plasma are implanted and the operating conditions must therefore be carefully adjusted to favor one ion species, e.g., O_2^+ in SPIMOX or H_2^+ in ion-cut/bonding. It has been shown that by adjusting plasma parameters such as pressure, a single ion species can be preferentially enhanced to accomplish single species PIII. Under these conditions, the efficiency and time saving of the PIII process compared to conventional beam-line ion implantation is evident, particularly for 200- and 300-mm silicon wafers.

Manuscript received March 18, 1998. This work was supported by City University Strategic Grant 7000730 and Hong Kong Research Grants Council Earmarked Grants 9040220 and 9040332.

Z.-N. Fan, Q.-C. Chen, and P. K. Chu are with the Department of Physics and Materials Science, City University of Hong Kong, Kowloon, Hong Kong (e-mail: paul.chu@cityu.edu.hk).

C. Chan is with the Department of Electrical and Computer Engineering, Northeastern University, Boston, MA 02115 USA.

Publisher Item Identifier S 0093-3813(98)09645-3.

Another requirement that must be met in SOI fabrication by PIII is that the mean free path of the ions must be larger than the thickness of the plasma sheath, otherwise collision in the sheath will reduce the implantation energy and consequently broaden the in-depth distribution. The process windows of SOI synthesis by PIII have been discussed [16] and several conclusions are drawn. First of all, the implantation current is very large, thereby necessitating a high current dc power supply and modulator. The high implantation current also raises the temperature of the silicon wafer significantly during PIII, and sample cooling is a big issue especially for the ion-cut process. Even in the case of SPIMOX that requires a substrate temperature of 600 °C, the large ion flux can create so much heat that the wafer can be melted during PIII. The design of a high voltage sample stage that can be heated and cooled presents tremendous engineering difficulties, and it is much easier to tackle the problem by resorting to low pressure PIII conditions which automatically guarantee a collisionless environment for mono-energetic implantation. In low pressure, the current impacting the sample is reduced thereby alleviating the heating problem. Since PIII is such an efficient process, implantation can still be completed in a relatively short time retaining the throughput edge over conventional beam-line ion implantation. However, the mean free path in the low pressure regime can be quite large [16] and comparable to the size of the vacuum chamber. If the plasma sheath reaches the chamber wall, a stable plasma cannot be sustained. Hence, it is important to determine the various parameters for low pressure PIII. In this paper, we formulate a theoretical model to simulate low pressure PIII and present experimental data to determine the process window of hydrogen PIII used in the ion-cut/wafer bonding technique to fabricate SOI.

II. Low Pressure PIII Modeling

A. DC Threshold Voltage

An important parameter is the threshold voltage V_{DC} in the dc PIII mode. If the applied voltage V_0 goes beyond V_{dc}, the dc (or static) sheath edge will hit the chamber wall or the plasma source and the plasma will extinguish. Taking a slab geometry, the collisionless sheath thickness can be calculated

0093–3813/98$10.00 © 1998 IEEE

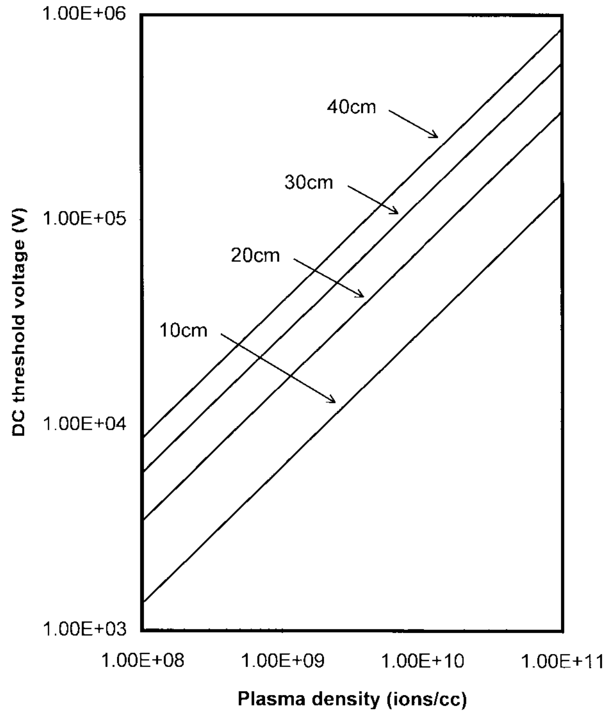

Fig. 1. DC threshold voltage versus H^+ plasma density for different chamber size (cm).

by Child's law [17]

$$\begin{cases} s = \sqrt{\frac{4}{9}\varepsilon_0\left(\frac{2e}{M}\right)^{1/2}\frac{V_0^{3/2}}{J_0}} \\ J_0 = en_0u_b \\ u_b = \sqrt{\frac{eT_e}{M}} \end{cases} \tag{1}$$

where s, J_0, u_b, T_e, M, e, and ε_0 are the sheath thickness, plasma ion current density, Bohm velocity, electron temperature, ion mass, electronic charge, and permittivity of free space, respectively. To limit the sheath in the chamber of which the length is L

$$V_0 \leq V_{\mathrm{DC}} = \left[\frac{9}{4\varepsilon_0}\left(\frac{eM}{2}\right)^{1/2} n_0 u_b L^2\right]^{2/3}. \tag{2}$$

Fig. 1 depicts the threshold voltage versus hydrogen plasma density for different chamber length. H^+ is the dominant ion in the calculation. The electron temperature T_e is set to 3 eV. V_{DC} is the maximum voltage at which the PIII system can be operated in a stable condition.

B. Model for Pulsed Implantation

In the pulsed PIII mode, if the voltage V_0 applied to the sample stage is less than the dc threshold voltage V_{DC}, the sheath will never hit the chamber wall regardless of the pulse duration. Even though the pulse voltage is higher than V_{DC}, the plasma still may not extinguish if the pulse is turned off before the sheath edge dynamically propagates to the chamber wall where the RF source is. Thus, there are two interrelated parameters, the threshold pulse voltage V_{pl} and the threshold pulse duration T_{pl}. Every PIII system with a certain chamber size and plasma properties has its T_{pl}–V_{pl} characteristic curve in the operational phase space. If a working point is above that curve, the plasma cannot be sustained and implantation will be prematurely terminated as the plasma goes off. The T_{pl}–V_{pl} curves can be calculated based on our model.

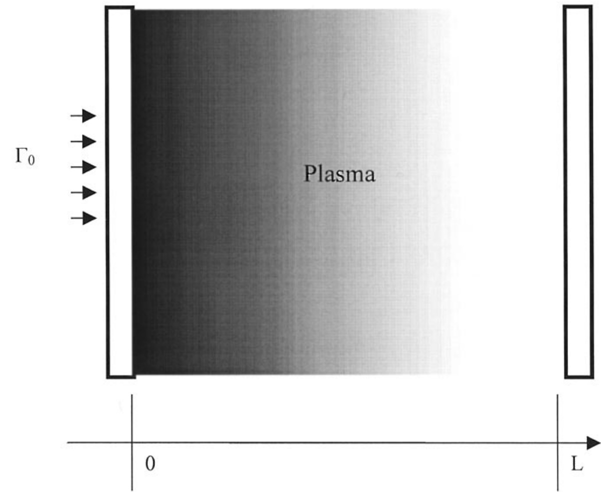

Fig. 2. Schematic diagram of one-dimensional PIII model.

When a pulsed voltage V_0 is applied to the sample stage, electrons are expelled from the region adjacent to the sample stage and leave the ion-matrix sheath [18] in a very short time on the order of the inverse electron plasma frequency ω_{pe}. In a low plasma density (10^8–10^{10} ions/cm^3) condition, this time scale is around 10^{-8}–10^{-9} s. Next, the sheath edge expands as ions are accelerated toward the sample stage. To derive the dynamic sheath propagation equation [19], [20], several assumptions are made here. The sheath is collisionless since the selected implantation pressure is around 0.4 mtorr. The time to form the Child's law sheath is much shorter than that for the sheath to make an observable movement. Therefore, we can use quasi-static Child's law [21] to describe the sheath propagation

$$\begin{cases} s = \sqrt{\frac{4}{9}\varepsilon_0\left(\frac{2e}{M}\right)^{1/2}\frac{V_0^{3/2}}{J}} \\ J = en_s\left(u_b + \frac{ds}{dt}\right) \end{cases} \tag{3}$$

where the sheath thickness s, ion current density J, and plasma density n are functions of time t.

To solve (3), we need the initial condition and plasma density distribution $n(x, t)$. Using the model in Fig. 2, the plasma enters from the left side with a constant flux Γ_0 and a negative voltage is applied to the right side. Assuming that there is no ion creation in the space, the plasma density distribution $n(x, t)$ satisfies the diffusion equation [22] at all time

$$\frac{dn(x, t)}{dt} - D\frac{d^2n(x, t)}{dx^2} = 0 \tag{4}$$

where D is the ambipolar diffusion coefficient. The initial plasma density $n(x, 0)$ can be solved without time dependence

$$-D\frac{d^2n(x, 0)}{dx^2} = 0. \quad (5)$$

The solution is a linear decay across the plasma region

$$n(x, 0) = \frac{\Gamma_0}{D}(L - x) + B. \quad (6)$$

To determine the coefficient B, we must investigate the boundary condition. Before the voltage is applied, there is a very thin sheath around the right wall. This initial sheath thickness is several Debye lengths and can be omitted in our calculation. The ion flux lost to the right wall must be

$$\Gamma = n_s u_b. \quad (7)$$

In a steady state, Γ must be equal to Γ_0. Thus, n_s is assigned to be the plasma density at the right side $n(L, 0)$ since the initial sheath thickness is neglected. The initial plasma density across the region is

$$n(x, 0) = \frac{\Gamma_0}{D}(L - x) + \frac{\Gamma_0}{u_b}. \quad (8)$$

We assume that an abrupt negative voltage $-V_0$ is applied to the right wall and the matrix sheath is formed in a very short time before the ions go into motion. Hence, the ion distribution still satisfies (8). The matrix sheath thickness s_0 can be calculated by solving Poisson's equation [18]

$$\frac{d^2\phi}{dx^2} = -\frac{e}{\varepsilon_0}n_i. \quad (9)$$

Substituting (8) into the right-hand side of (9), we obtain

$$\phi = -\frac{e}{\varepsilon_0}\left[\frac{1}{6}\frac{\Gamma_0}{D}x^3 + \frac{1}{2}\frac{\Gamma_0}{u_b}x^2\right]. \quad (10)$$

Setting $\phi = -V_0$, the ion matrix sheath thickness satisfies the following:

$$V_0 = \frac{e}{\varepsilon_0}\left[\frac{1}{6}\frac{\Gamma_0}{D}s_0^3 + \frac{1}{2}\frac{\Gamma_0}{u_b}s^2\right]. \quad (11)$$

By applying the initial and boundary conditions, the sheath propagation and ion current can be solved from the dynamic sheath equation (3) and diffusion equation (4). Adopting the criterion that the sheath edge propagates to the left side, we can derive the T_{pl}–V_{pl} characteristic curves.

C. Simulation Results

The equations can be solved numerically by the finite difference method (FDM) assuming H^+ to be the dominant ion species in the plasma. The electron temperature is assumed to be 3 eV and the Bohm velocity is thus 1.7 $\times 10^4$m/s. The relationship of the threshold pulse T_{pl} versus the threshold voltage V_{pl} is systematically studied for different plasma diffusion coefficient D, ion flux Γ_0, and chamber size L. Figs. 3–5 depict the T_{pl}–V_{pl} curves under various plasma conditions. In a fast diffusion system, the plasma sheath expands rapidly and the time needed to reach equilibrium is short. Fig. 3 displays V_{pl} and T_{pl} for different diffusion coefficients. The calculation assumes that the ion flux at the left side is 8.5 $\times$ $10^{18}\text{m}^{-2}\text{s}^{-1}$ and that the chamber size is 0.5 m. The dc threshold voltage V_{DC} in such a system is 42.7 kV. The implantation voltage from 45–100 kV is investigated in Fig. 3. For the same implantation voltage, a longer pulse width can

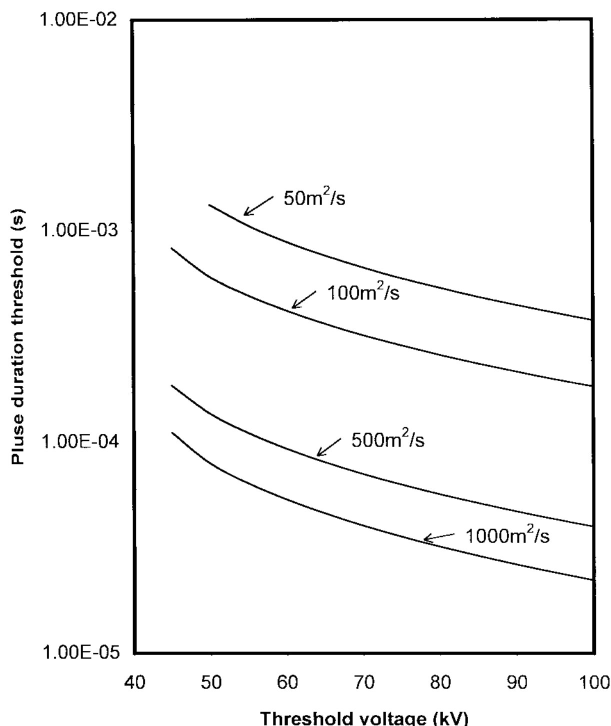

Fig. 3. Threshold pulse duration versus threshold voltage for different diffusion coefficients in pulsed PIII.

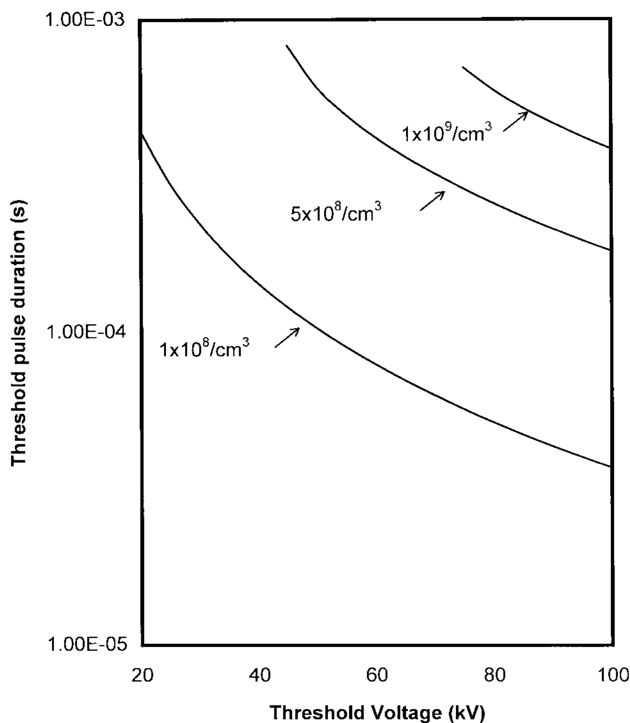

Fig. 4. Threshold pulse duration versus threshold voltage for different ion fluxes in pulsed PIII.

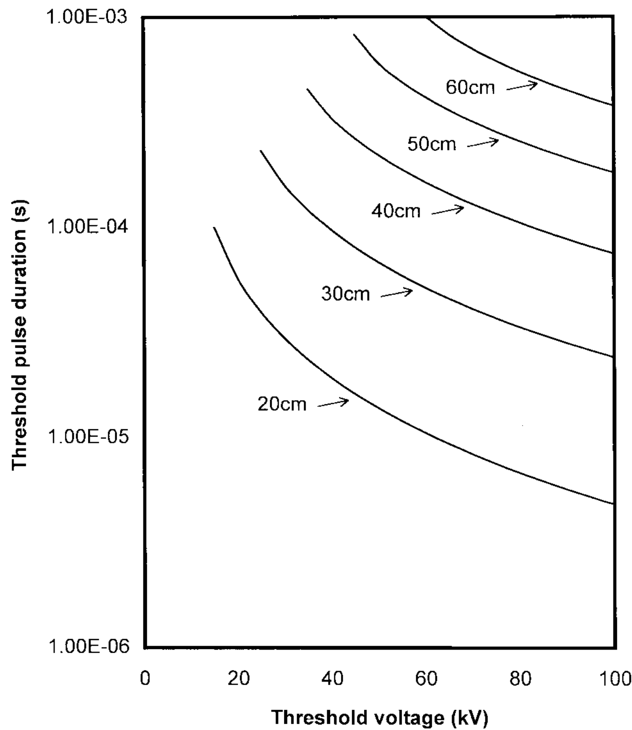

Fig. 5. Threshold pulse duration versus threshold voltage for different chamber size in pulsed PIII.

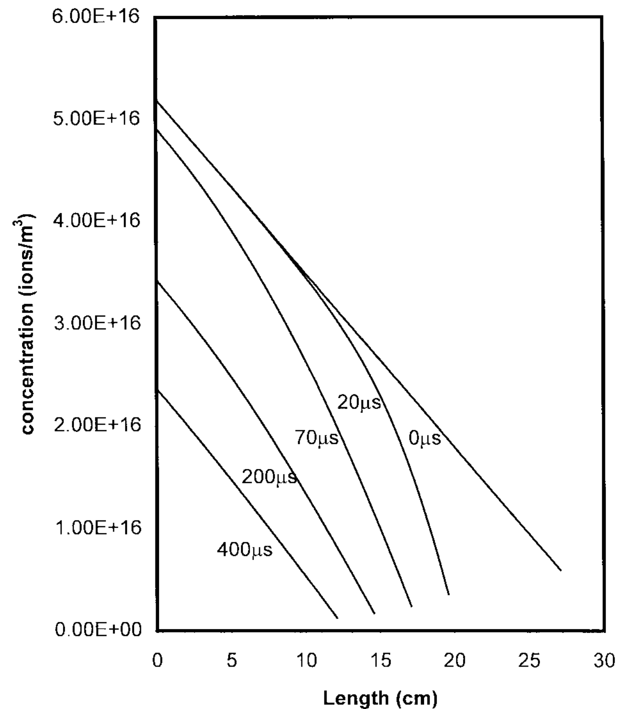

Fig. 6. Evolution of the plasma density distribution with implantation time.

be tolerated for a smaller diffusion coefficient. The threshold pulse duration ranges from 830 μs to 180 μs as the threshold voltage changes from 45–100 kV for a diffusion coefficient of 100 m^2/s. Fig. 4 illustrates the relationship between the maximum pulse duration and threshold voltage for different ion fluxes Γ_0. The chamber size is 0.5 m and the plasma diffusion coefficient is 100 m^2/s in this derivation. It is obvious that an efficient plasma source capable of a high plasma creation rate is beneficial to long pulse PIII. Fig. 5 shows the pulse duration limitation versus the threshold voltage for a vacuum chamber of different sizes. If there is no electrical arcing between the chamber wall and the sample stage, i.e., the vacuum chamber and stage is sufficiently isolated, a small chamber 20 cm in length can sustain 100 kV implantation if the pulse duration is limited to several ms.

D. Sheath Interference from Plasma Source

In the above discussion, the ion flux from the left side is set to be constant. In reality, the plasma creation depends upon ionizing collisions between electrons and neutral atoms, and a smaller electron density will result in the reduction in the plasma intensity. It is obvious that the plasma will extinguish if the sheath expands to the plasma source region because there are almost no electrons in the sheath region. Even if the sheath does not touch the plasma source, the plasma intensity will still diminish as the sheath edge approaches the plasma source. Fig. 6 depicts the evolution of the plasma density distribution when -20 kV is applied to the right side. The chamber size is 0.5 m and the ion flux is $1.7 \times 10^{19} m^{-2} s^{-1}$. Our results show that even though the plasma density is higher toward the source (left side) at any given time, the bulk plasma density decreases as the sheath propagates, i.e., lower density at a longer implantation time. Since the bulk plasma is neutral, the electron density is equal to the ion density and decreases as the sheath propagates. Thus, in a system where the plasma source and sample are in the same chamber, the sheath propagation decreases the electron density and consequently reduces the plasma intensity. The reduction in the plasma intensity will in turn accelerate the sheath expansion. The system thus falls into a self-perpetuating mode in which the sheath continues to expand faster and is much thicker than that shown in the previous calculation. In some cases, the system cannot reach equilibrium and the plasma extinguishes quickly. Fig. 6 also shows that the plasma density during implantation is much lower than the static plasma density measured by a Langmuir probe without the high voltage.

III. Experimental Results and Discussion

To further investigate low pressure PIII, experiments were conducted. The PIII equipment used in this work has been described in details elsewhere [16]. Hydrogen PIII is a temperature sensitive process and therefore requires low pressure PIII [13]. It is used to investigate three important parameters: pulse width, implantation voltage, and gas pressure.

A. Pulse Width

For mono-energetic implantation in the collisionless regime, the width of the voltage pulse should be as long as possible, provided that the average current is low enough not to raise the substrate temperature significantly during PIII. However, a long pulsing time will allow the plasma sheath to expand to the chamber wall causing instability and eventually extinction of the plasma. Hence, the current-voltage characteristic for

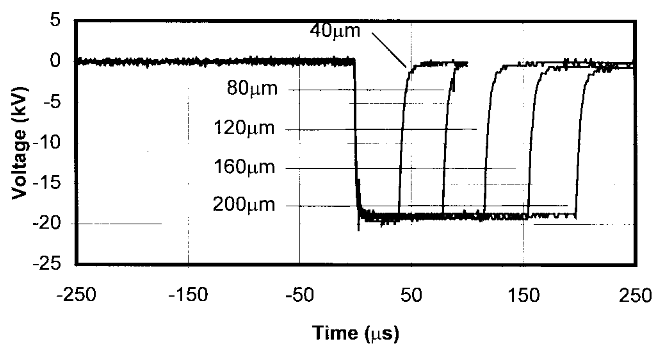

(a)

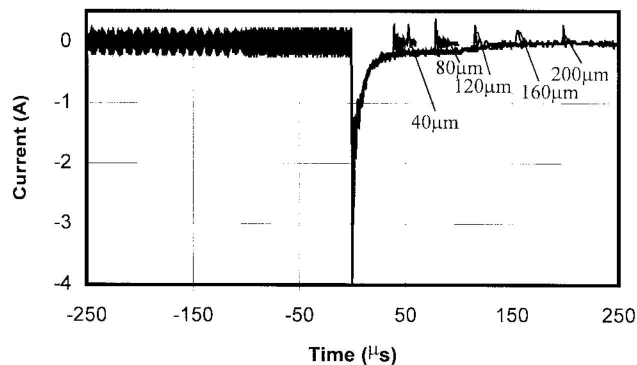

(b)

Fig. 7. (a) Voltage waveforms and (b) current waveforms of different pulse widths for −20 kV implantation at 900 W RF and 0.3 mtorr pressure.

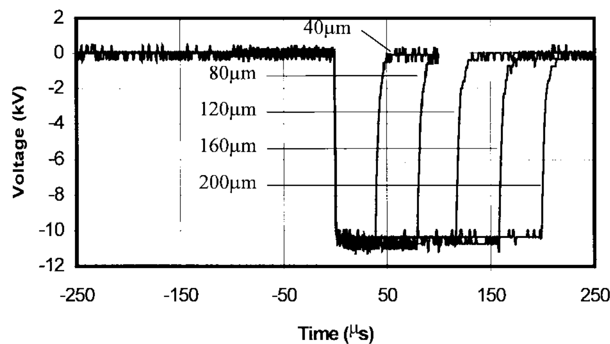

(a)

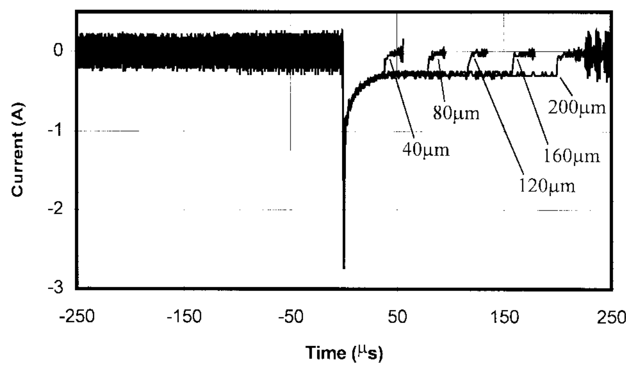

(b)

Fig. 8. (a) Voltage waveforms and (b) current waveforms for different pulse widths for 10kV implantation at 900W RF and 0.3 mtorr pressure.

different pulse durations must be investigated. Fig. 7 exhibits the current and the voltage waveforms of different pulse widths for hydrogen PIII. The implantation voltage, gas pressure, and RF power were −20 kV, 0.3 mtorr, and 900 W, respectively. The current waveform observed for a 200 μs pulse is very interesting and five characteristic periods can be identified.

1) *Peak Current Period*: It corresponds to the 2 μs rise time of the voltage waveform. Electrons are expelled as the voltage is increased. The current reaches a high value rapidly depending on the voltage slew rate. In our results, the peak current is about 4A and much higher than the average implantation current.
2) *Propagation Period*: In this stage, the sheath propagates dynamically [23]. The sheath propagation speed is high at the beginning of the pulse and diminishes subsequently. The current decreases as the sheath thickness increases according to Child's law (3). The duration of this sheath expansion is about 45 μs in our implantation condition.
3) *Constant Current Period*: From 45–105 μs, the plasma is relatively stable. Ions are fully accelerated by the sheath into the silicon wafer. In case of low voltage implantation depicted in Fig. 8, the sheath stops expanding and the current is constant from here to an infinite time. Nonetheless, a small current decline can be observed in Fig. 7 because the bulk plasma density decreases during sheath expansion.
4) *Decay Period*: The sheath approaches closely to the plasma source after 105 μs and violently affects the plasma excitation. Since very few electrons are in the sheath region at this stage, ion creation drops precipitously. The implantation current falls to zero at 140 μs.
5) *Extinction Period*: In this period, the sheath edge finally reaches the top chamber wall. During this phase, the plasma flashes violently in the chamber and eventually goes off. The chamber becomes dark and no ions are created or implanted. The implantation current is zero.

Therefore, in order to attain plasma stability and avoid plasma extinction, the pulse duration must be short.

In low voltage PIII, only the first three periods can be observed. Fig. 8 shows the waveforms for −10 kV implantation. The other implantation parameters are kept the same. After 45 μs, current reduction is not apparent and the implantation current is constant until the end of the pulse at 200 μs.

B. Pulse Voltage

Plasma sheath propagation strongly depends on the applied voltage as the sheath thickness increases with the implantation voltage [1]. As discussed previously, the bulk plasma density is lower in higher voltage implantation because the sheath edge is closer to the plasma source. Fig. 9 displays the waveforms at different voltages: −10, −15, −20, and −25 kV. The gas pressure is 0.4 mtorr. The waveform obtained at −25 kV has the highest current peak but the lowest implantation current after the propagation period. The current begins to drop after 80 μs. For the waveforms acquired at −10 kV, the current

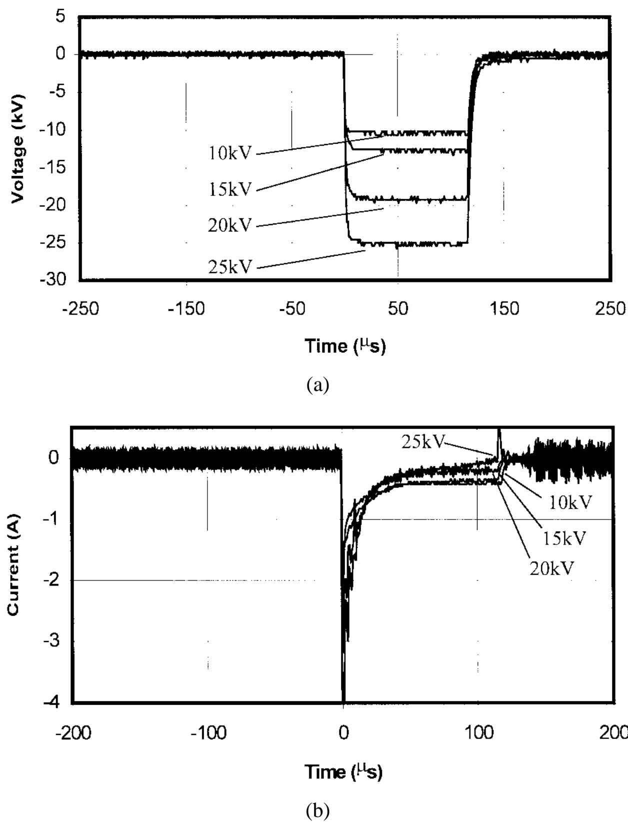

Fig. 9. (a) Voltage waveforms and (b) current waveforms at different implantation voltages at 900 W RF and 0.3 mtorr pressure.

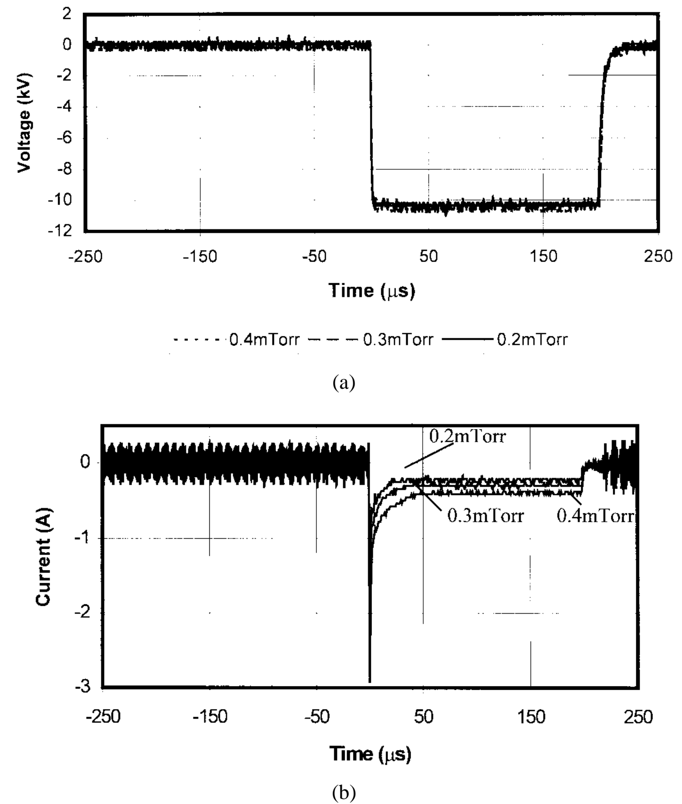

Fig. 10. (a) Voltage waveforms and (b) current waveforms at different pressure for -10 kV implantation at 900 W RF.

reaches an equilibrium when the sheath propagation stops and no obvious change is found after 50 μs. In Fig. 9, the current evolution has an inverse relationship with the implantation voltage. That is, at a higher voltage, the implantation current is lower in the constant current period. We attribute it to the lower plasma creation rate during high voltage implantation since the area of the sheath edge is almost equal to the chamber cross-sectional area after the sheath hits the chamber side wall.

C. Gas Pressure

The plasma density is essentially proportional to the gas pressure in the low-pressure (<1 mtorr) region [16]. Therefore, increasing the gas pressure will boost the implantation current. The current and voltage waveforms of -10 kV implantation at different pressure are displayed in Fig. 10. Though the plasma density at 0.4 mtorr pressure is higher and the sheath is thinner, the time the sheath takes to reach its steady state is longer than that at 0.2 and 0.3 mtorr. Fig. 11 shows the time it takes to achieve a stable current from the start of the voltage pulse for different gas pressure for -10 kV implantation as derived from Fig. 10.

The waveforms at higher voltage -20 kV are illustrated in Fig. 12. When the pressure decreases to 0.2 mtorr, stability can no longer be maintained and the plasma goes off. No current is detected. The two small peaks in the current waveform correspond to charging during the voltage rise and discharging during the voltage fall.

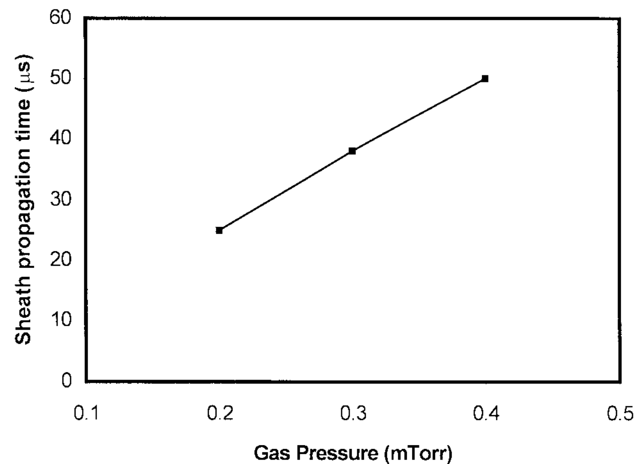

Fig. 11. Sheath propagation time for -10 kV implantation at different gas pressure.

D. DC Implantation

DC PIII is a subset of pulsed PIII in which the pulse width is infinitely long. The dc implantation current can be written as

$$I = enu_b A \tag{12}$$

where A is the sheath area. Fig. 13 depicts the relationship of the implantation current versus the applied voltage in dc implantation. The experiment was performed using 900 W RF power and at 0.4 mtorr working pressure. The current

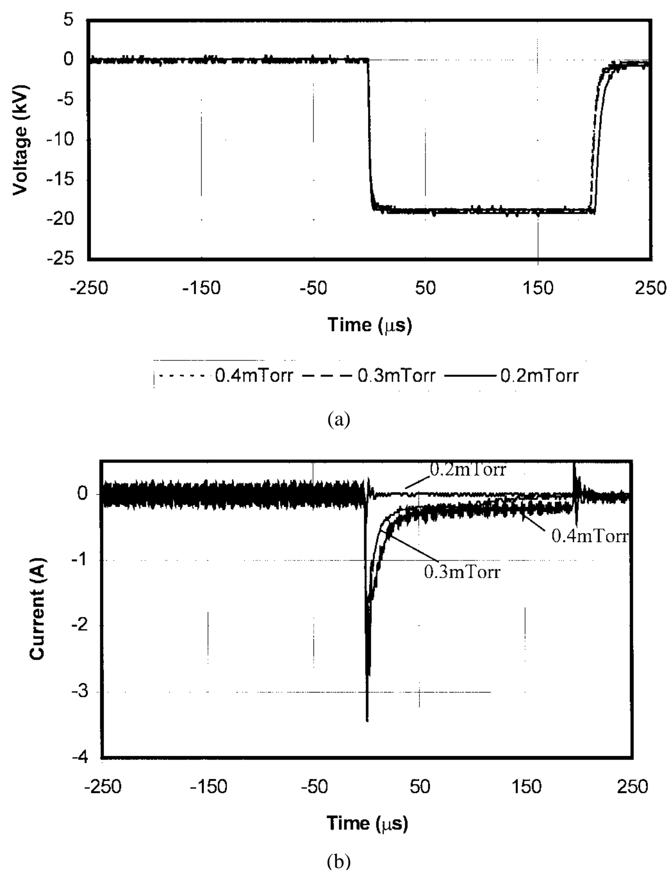

Fig. 12. (a) Voltage waveforms and (b) current waveforms for −20 kV implantation at 900 W RF and different pressure.

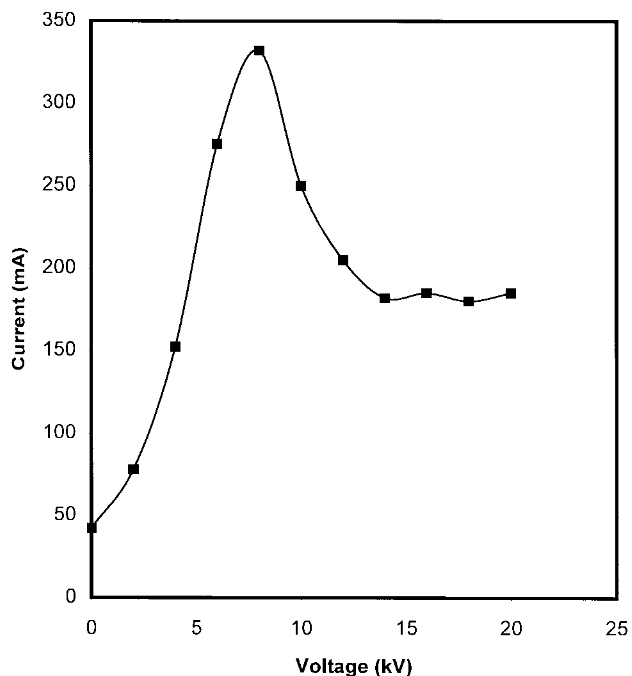

Fig. 13. Current-voltage relation for dc implantation.

increases monotonically with voltage at the low voltage region but shows a sudden drop at −8 kV. Above −12 kV, the implantation current does not vary significantly with voltage. When the voltage goes beyond −20 kV, the current decreases rapidly and the plasma extinguishes. The maximum current is 330 mA at −8 kV.

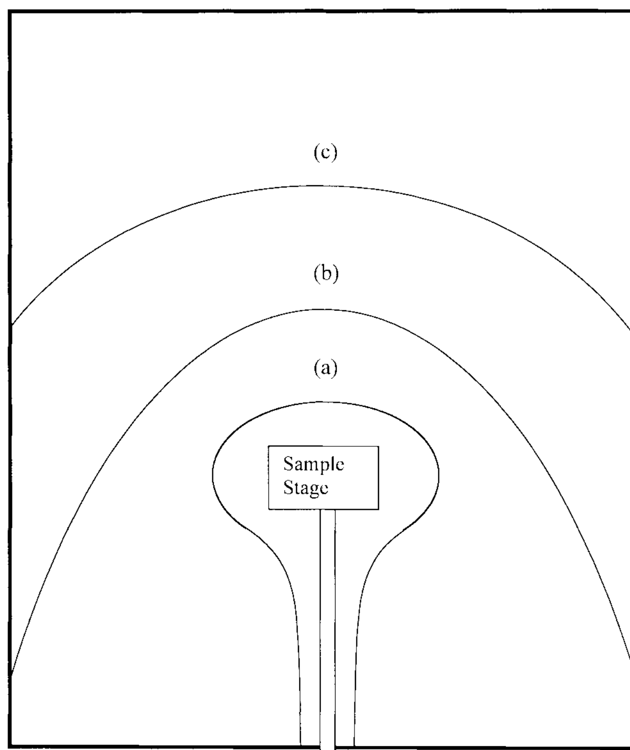

Fig. 14. Sheath evolution with voltage for dc implantation.

To explain the above results, the sheath evolution as the voltage is increased is illustrated in Fig. 14. Using (12), the current is a function of the area of the sheath edge if the Bohm velocity u_B and plasma density n do not change with the voltage. The low voltage sheath is like curve (a) in Fig. 14. The sheath region expands, and the current goes up as the voltage is raised. Since the plasma density is highest directly above the wafer stage in a down-stream plasma system and the distance between the stage and chamber top (RF source) is larger than that between the stage and the chamber side wall, the sheath must hit the side wall first (curve (b) in Fig. 14). The sheath represented by curve (b) in Fig. 14 has the maximum area and consequently delivers the maximum current (corresponding to −8 kV in Fig. 13). When the voltage is increased further, the sheath area collapses into curve (c) that has a smaller surface area than curve (b). As the sheath edge approaches the source region on top [post curve (c)], the sheath shape remains unchanged and the implantation current does not vary significantly. Beyond −20 kV, the static sheath reaches the plasma source. The plasma can no longer be sustained and the current drops to zero.

IV. SUMMARY

Low pressure PIII is characterized by the current-voltage characteristics. The threshold pulse duration and voltage for pulsed implantation are derived using our model. Experimentally, it is observed that the implantation current decreases with the pulse time, and plasma extinction is observed at

high voltage, low pressure, and long pulse implantation. At the same voltage, the implantation current increases with the gas pressure. Our results show an interesting phenomenon that the absolute implantation current at the constant current period decreases as the voltage increases. It is due to the change in the plasma creation efficiency as the sheath propagates away from the sample stage.

REFERENCES

[1] P. K. Chu, S. Qin, C. Chan, N. W. Cheung, and L. A. Larson, "Plasma immersion ion implantation—A fledgling technique for semiconductor processing," *Mat. Sci. Eng.: Reports,* vol. R17, no. 6/7, pp. 207–280, 1996.

[2] J. V. Mantese, I. G. Brown, N. W. Cheung, and G. A. Collins, "Plasma immersion ion implantation," *MRS Bulletin,* vol. 21, no. 8, pp. 52–56, 1996.

[3] P. K. Chu, N. W. Cheung, and C. Chan, "Recent applications of plasma immersion implantation," *Semicond. Int.,* vol. 6, pp. 165–172, June 1996.

[4] N. W. Cheung, "Plasma immersion ion implantation for semiconductor processing," *Materials Chem. Phys.,* vol. 46, pp. 132–139, 1996.

[5] S. Qin and C. Chan, "Plasma immersion ion implantation doping experiments for microelectronics," *J. Vac. Sci. Technol. B,* vol. 12, no. 2, pp. 962–968, 1994.

[6] B. Mizuno, H. Nakaoka, M. Takase, A. Hori, I. Nakayama, and M. Ogura, "Plasma doping and plasma-less doping of semiconductor," *Ext. Abstract 1995 Int. Conf. Solid State Develop. Mat.,* Osaka, Japan, 1995, p. 1041.

[7] J. D. Bernstein, S. Qin, and C. Chan, "Hydrogenation of polycrystalline silicon thin film transistors by plasma ion implantation," *IEEE Electron Device Lett.,* vol. 16, no. 10, pp. 421–423, 1995.

[8] J. Min, P. K. Chu, Y. C. Cheng, J. B. Liu, S. Im, S. Iyer, and N. W. Cheung, "Buried oxide formation by plasma immersion ion implantation," *Mat. Chem. Phys.,* vol. 40, no. 3, pp. 219–222, 1995.

[9] J. B. Liu, S. S. K. Iyer, C. M. Hu, N. W. Cheung, R. Gronsky, J. Min, and P. Chu, "Formation of buried oxide in silicon using separation by plasma implantation of oxygen (SPIMOX)," *Appl. Phys. Lett.,* vol. 67, no. 16, pp. 2361–2363, 1995.

[10] J. Min, P. K. Chu, Y. C. Cheng, J. Liu, S. S. Iyer, and N. W. Cheung, "Nucleation mechanism of SPIMOX (separation by plasma implantation of oxygen)," *Surf. Coatings Technol.,* vol. 85, no. 1–2, pp. 60–63, 1996.

[11] X. Lu, S. S. K. Iyer, J. B. Liu, C. M. Hu, N. W. Cheung, J. Min, and P. K. Chu, "Separation by plasma implantation of oxygen to form silicon on insulator," *Appl. Phys. Lett.,* vol. 70, no. 13, pp. 1748–1750, 1997.

[12] P. K. Chu, X. Lu, S. S. K. Iyer, and N. W. Cheung, "A new way to make SOI wafers," *Solid State Technol.,* vol. 49, no. 5, pp. S9–S12, 1997.

[13] X. Lu, N. W. Cheung, M. D. Strathman, P. K. Chu, and D. Doyle, "Hydrogen induced silicon surface layer cleavage," *Appl. Phys. Lett.,* vol. 71, no. 13, pp. 1804–1806, 1997.

[14] S. S. K. Iyer, X. Lu, J. B. Liu, J. Min, Z. N. Fan, P. Chu, C. M. Hu, and N. W. Cheung, "Separation by plasma immersion of oxygen (SPIMOX) operational phase-space," *IEEE Trans. Plasma Sci.,* vol. 25, pp. 1128–1135, Oct. 1997.

[15] X. Lu, S. S. K. Iyer, C. M. Hu, N. W. Cheung, J. Min, Z. N. Fan, and P. K. Chu, "Ion-cut silicon-on-insulator fabrication with plasma immersion ion implantation," *Appl. Phys. Lett.,* vol. 71, no. 19, pp. 2767–2769, 1997.

[16] P. K. Chu, S. Qin, C. Chan, N. W. Cheung, and P. K. Ko, "Instrumental and process considerations for the fabrication of silicon-on-insulators (SOI) structures by plasma immersion ion implantation," *IEEE Trans. Plasma Sci.,* vol. 26, pp. 79–84, Feb. 1998.

[17] M. A. Lieberman and A. J. Lichtenberg, *Principles of Plasma Discharges and Materials Processing.* New York: Wiley, 1994.

[18] J. R. Conrad, "Sheath thickness and potential profiles of ion-matrix sheath for cylindrical and spherical electrodes," *J. Appl. Phys.,* vol. 62, no. 3, pp. 777–779, 1987.

[19] M. A. Lieberman, "Model of plasma immersion ion implantation," *J. Appl. Phys.,* vol. 66, no. 7, pp. 2926–2929, 1989.

[20] J. T. Scheuer, M. Shamin, and J. R. Conrad, "Model of plasma source ion-implantation in planar, cylindrical, spherical geometries," *J. Appl. Phys.,* vol. 67, no. 3, pp. 1241–1245, 1990.

[21] M. A. Lieberman, "Analytical solution for capacitive RF sheath," *IEEE Trans. Plasma Sci.,* vol. 16, pp. 638–644, Dec. 1988.

[22] F. F. Chen, *Introduction to Plasma Physics and Controlled Fusion, Vol.: Plasma Physics.* New York: Plenum, 1984.

[23] M. Shamin, J. T. Scheuer, and J. R. Conrad, "Measurement of spatial and temporal sheath evolution for spherical and cylindrical geometries in plasma source ion-implantation," *J. Appl. Phys.,* vol. 69, no. 5, pp. 2904–2908, 1991.

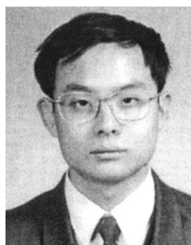

Zhi-Neng Fan received the B.S. degree in physics in 1992 and the M.S. degree in materials science in 1996, from Fudan University. He received the Ph.D. degree in plasma immersion ion implantation under the supervision of Prof. P. K. Chu at the City University of Hong Kong in 1998.

His research interests include plasma immersion ion implantation, separation by plasma implantation of oxygen, ion-cut, thin film transistor processing, and plasma enhanced oxidation.

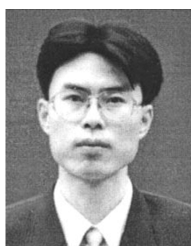

Qing-Chuan Chen was born in Zhejiang, China, on March 24, 1970. He received the B.S. degree in computer-aided machine design and manufacturing from Zian Jiaotong University, China, in 1992.

He joined Southwestern Institute of Physics, China, in 1992 and was appointed Assistant Engineer and Engineer in 1993 and 1997, respectively. He was also the Vice-Director of the Ion Beam Development and Application Center of Southwestern Institute of Physics. He is currently working as a Research Assistant in the Plasma Laboratory at the City University of Hong Kong. His research interests include plasma immersion ion implantation, as well as other ion beam implantation technologies and hardware.

Paul K. Chu (M'97), for a photograph and biography, see p. 180 of the April 1998 issue of this TRANSACTIONS.

Chung Chan (S'79–M'81–SM'88–F'97), for photograph and biography, see this issue, p. 1590.